Solid State Science and Technology, Vol. 24, No 1 (2016) 189-197
ISSN 0128-7389 | *http://journal.masshp.net*

MICROSTRUCTURE AND DIELECTRIC PROPERTIES OF PARALLEL EVOLUTION ON $Ni_{0.3}Zn_{0.7}Fe_2O_4$ NANOPARTICLES

Mohd Noor Mat[1], M. K. Halimah[2], W. M. D. W. Yusoff[3], H. Mansor[4] and T. I. T. M. Aiman[5]

[1]*Kolej Matrikulasi Kelantan, 16810 Selising, Pasir Puteh, Kelantan.*

[2]*Physic Department, Faculty of Science, University Putra Malaysia, 43400 Serdang, Selangor*

[3]*Centre of Foundation Studies for Agriculture Science, University of Putra Malaysia, 43400 Serdang, Selangor*

[4]*Institute of Advanced Technology (ITMA), University of Putra Malaysia, 43400 Serdang, Selangor, Malaysia*

[5]*Mechanical Engineering Department, Korea University, Korea*

Corresponding author: mohdnoormatkms@yahoo.com

ABSTRACT

Nickel substituted zinc ferrite nanoparticles of the composition $Ni_{0.3}Zn_{0.7}Fe_2O_4$ have been synthesized by the solid state method. The samples were characterised by X-ray diffraction, Field Emission Scanning electron microscopy (FESEM), and dielectric studies. The X-ray diffraction patterns confirm the synthesis of single crystalline phase of $Ni_{0.3}Zn_{0.7}Fe_2O_4$ nanoparticles. An improvement in the crystal structure is observed when samples were annealed at 1173 K to 1573 K. FESEM reveals that the sample has well dispersed nanoparticles. The dielectric constant decreases with increased frequency, the dispersion at low frequency range are follows the Maxwell-Wegner interfacial polarization.

Keyword: Nickel zinc ferrite(NZF); annealing; X-ray diffraction; Field Emission Scanning electron microscopy; X-ray and dielectric properties;

INTRODUCTION

Sintering is commonly defined as a process thermally activated, in which compacted powder density and develop a microstructure with useful properties [1]. An evolution of the sample is the same meaning with sintering or annealing of the sample. Nickel–Zinc(Ni-Zn) ferrites are ferrimagnetic materials with a large number of technological applications in telecommunications and entertainment electronics [2, 3, 4]. It is well known that ferrites are extremely sensitive to the manufacturing process, and hence that their properties are microstructurally dependent [1, 5]. Thus, to have a good

understanding of the behaviour of these materials, it is imperative to perform systematic investigations of their properties, in particular, the microstructural evolution during sintering (or their densification and grain growth kinetics). The microstructures developed during sintering are determined to a large extent by the powder characteristics (crystallite size and shape, size distribution, porosity, state of agglomeration, and chemical and phase composition) and by the green microstructure, which are intimately related to the processing method [6, 7, 8].

Generally, the electrical resistivity of ferrites decreases with the increase of temperature, which shows that ferrites have semiconductor behavior [5, 9, 10]. Ferrites have very high resistivity which is one of the considerations for microwave applications [3, 4]. The electrical properties of ferrites are sensitive to preparation method, sintering temperature, sintering time, the rate of heating and rate of cooling [1,11]. The study of electrical resistivity produces valuable information on behavior of free and localized electric charge carried in the sample [12, 13]. In Ni-Zn ferrite, at high temperature Zn^{2+} volatilization results the formation of Fe^{2+} ions, thereby increasing electron hopping and reducing resistivity [5, 9]. In this work, NZF were synthesized with different sintering temperature from 1173 K to 1573 K along 10 hours in the air. The effects of these parameters on the microstructural evolution are reported and qualitatively discussed in terms of the densification and grain growth kinetics.

EXPERIMENTAL

Ferrites particles of $Ni_{0.3}Zn_{0.7}Fe_2O_4$ were prepared using the dry method by mixing powder, Nickel Oxide, Iron Oxide and Zinc Oxide. Nickel Oxide (10 – 30nm size, 99% purity), Iron Oxide (20 – 40nm size, 99% purity) and Zinc Oxide (15 – 35 nm size, 99.5% purity) were used in this study. Composition and preparation method used in this study are following the method reported by Mat et al. (2015)[14]. After that, the sample pallet disc with the area, A, and the thickness, d, were sintered in the furnace for 10 hours at temperature 1173 K to 1573 K with intervals 100 K in air by parallel preparation. The surface morphology of the NZF was studied using FEI NOVA NanoSem 230 to reveal the microstructure of the sample product. XRD measurement is done for the sample by PAN analytical X'pert PRO diffractometer using Cu K_α radiation operated at 45 kV and 40 mA sources. Data collection is done in the range 20^o to 80^o in 2θ. The dielectric studies for the sample were carried out at 303 K in the frequency range 0.01 Hz to 3 MHz using a Novo Control dielectric spectrometer. The dielectric constant was measured using the relation, $\varepsilon = Cd/\varepsilon_o A$, where C is the capacitance of the sample in Farad, d and A are the thickness and the flat surface area of the sample and ε_o the permittivity of the free space (8.85×10^{-12} F/m).

RESULT AND DISCUSSION

X-ray Analysis

Fig. 1 shows the X-ray diffraction pattern of $Ni_{0.3}Zn_{0.7}Fe_2O_4$ and clearly the formation of spinel ferrite phase in sample. All the peaks in the diffraction pattern have been indexed and the refinement of lattice parameter was done using XPert HighScore

software. All the peaks are narrow and confirm the phase formation are crystals.

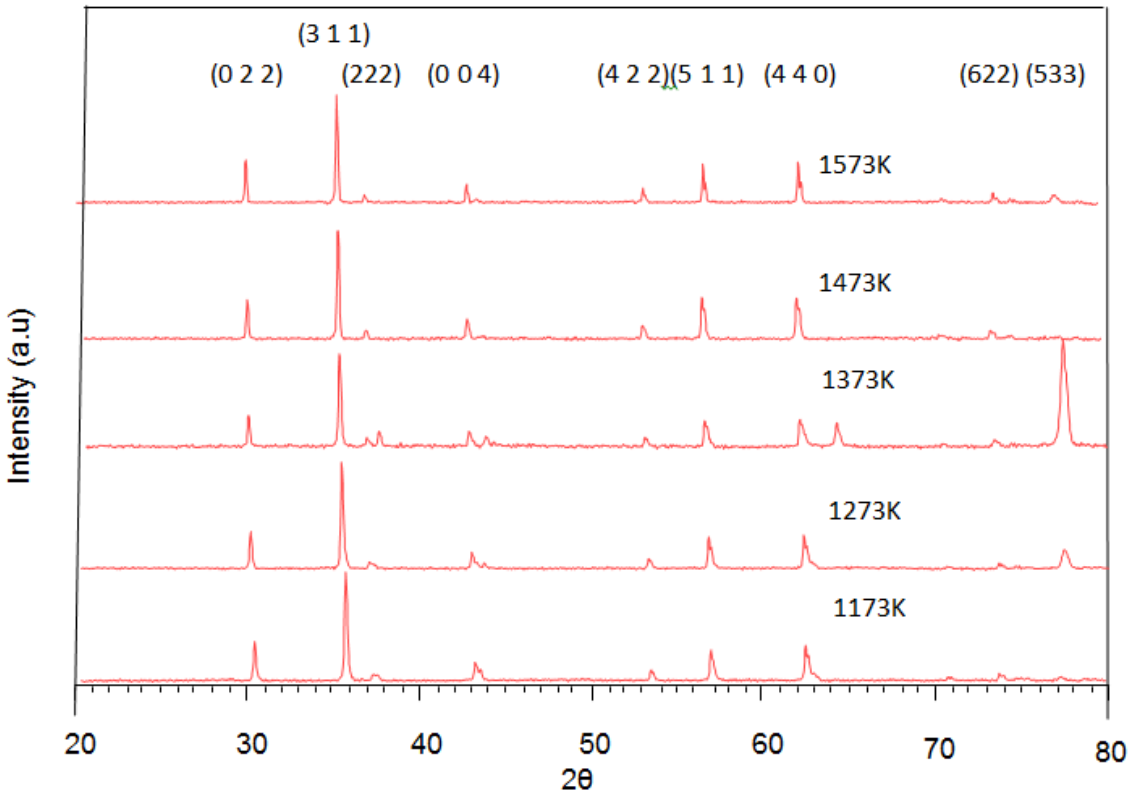

Figure 1: Phase formation of each sintering temperature of $Ni_{0.3}Zn_{0.7}Fe_2O_4$

Microstructure Analysis

Figure 2 (a) to (e) shows the FESEM image of NZF are observed at sintered at 1173 K to 1573 K. The images of grains are clear and the diameter of the grains can be measured. The distribution of position grains can be seen by arrangement in all samples studied. The grains arrangement in the sample can distinguish whether the sample is amorphous or crystal. The grain size is clearly different with same magnification (100000x).

When the sample was sinter with different temperatures, the size of the crystal were changes [15]. Thus, to have a good understanding of the behaviour of these materials, it is imperative to perform systematic investigations of their properties, in particular, the microstructural evolution during sintering [17]. The microstructures developed during sintering are determined to a large extent by the powder characteristics (crystallite size and shape, size distribution, porosity, state of agglomeration, and chemical and phase composition) and by the green microstructure, which are intimately related to the processing method [17].

From Figure 2 (a) to (e) can be seen the grain size that is clear and can be measured. By

using Item size measurement using Image J (IJ) by a transverse line per item and this measurement made several times per item. Before measurement made, determination of long sized is the first step by scale that exist on every figure or image from FESEM figure. This is aiming to get measure size according to the size that is real. The average diameter of grains sized of each sintering temperature can be recorded. At the same time, information about the average grain size of each sintering temperature can be used to explain the grain's growth kinetic of these samples. Figure 2 shows the linear growth of these samples.

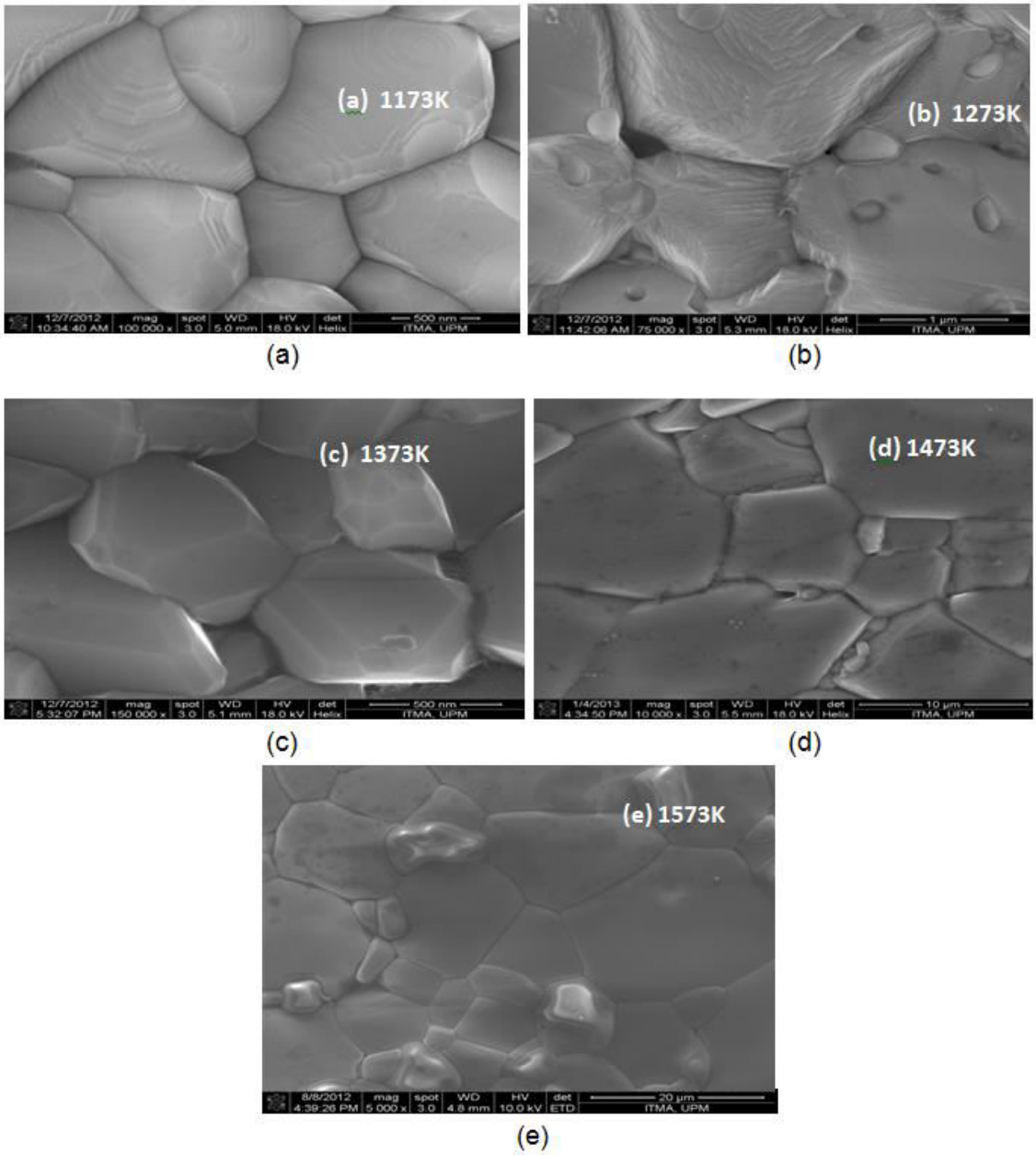

Figure 2: The FESEM microstructural evolution of the NZF samples of each sintering temperature

From Figure 3 shows that the average diameter decreases with the inverse of sintering temperature. The average grain size as a function of sintering can be used to predict the activation energy of grain growth of the materials [17]. The relation in between average grain size and activation energy is given by Equation (1):

$$\log d = \log d_o + \frac{E_d}{2.3R}\left(\frac{1}{T}\right) \quad (1)$$

where d is the average grain size of ferrites, E_d is activation energy of grain growth, d_o is average grain size independent with temperature, R is gas constant (8.314 JK^{-1} mol^{-1}) and T is sintering temperature respectively. Figure 3 shows two parts with two different slopes and will be used to calculate the activation energies of the grain grown. For the first part with two slopes, samples sintering from 1173K to 1373K, the activation energies is 205.0 ± 3.0 eV. Figure 5.3 (a) to (c) shows that the rate of grain growth is smaller. The small value of activation energy shows the diffusive motion of atoms in the ferrite samples is high. In view of the electrical properties, the potential barrier of an electron to hop to other state is low in these samples [17].

The high temperature sintered ferrite obtained higher activation energy of 454.0 ± 3.0 eV where the grain growth is faster. However, at low temperature sintered, the diffusive motion of atoms is low and the potential barrier of an electron to hop to other state is high in these samples. A large amount of energy is needed to excite the electron to cross over the barrier. The rapid increase in the grain size for high temperature sintered ferrite lead it to insulate properties [17].

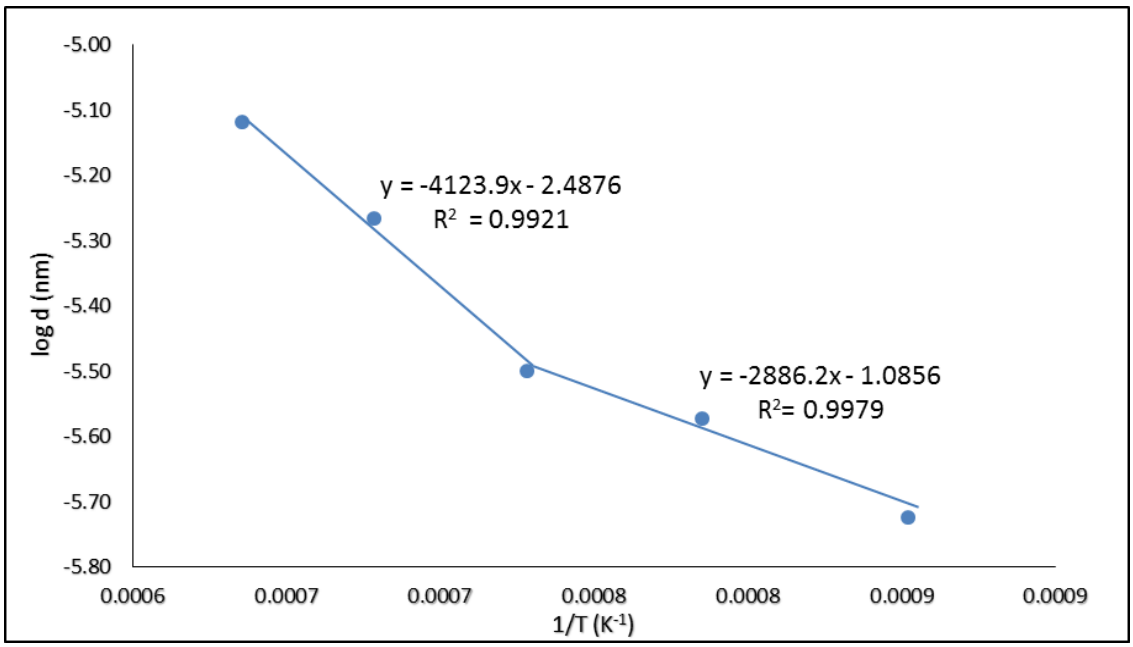

Figure 3: Plot diameter grains size versus reciprocal sintering temperatures

Dielectric Properties

A dielectric material is an electrical insulator that can be polarized by an applied electric field. An important property of a dielectric is its ability to support an electrostatic field while dissipating minimal energy in the form of heat [12, 13]. The lower the dielectric loss (the proportion of energy lost as heat), the more effective is a dielectric material [12, 13]. Metal oxides, in general, have high dielectric constants. The prime asset of high-dielectric-constant substances, such as aluminium oxide, is the fact that they make possible the manufacture of high-value capacitors with small physical volume. But these materials are generally not able to withstand electrostatic fields as intense as low-dielectric-constant substances such as air [18].

The dielectric relaxation phenomenon in NZF reflects the time dependence in the frequency response of a group of dipoles when interacting with an external applied electric field. When an external voltage is applied to the sample, the dipoles responsible to polarization are no longer able to follow the oscillations of the electric field at certain frequencies. The field reversal and the dipole reorientation become out of phase due to a dissipation of energy. Over a wide of frequency range, different types of polarization cause several dispersion regions and the critical frequency, characteristic of each contributing mechanism, depends on the nature of dipoles. The dissipation of energy, which is directly related to the dielectric losses, can be characterized by two factors [12, 13, 19]. First the losses associated with resonant processes, characteristics of the elastic displacing of ions and electrons. Second the dipolar losses, due to the reorientation of the dipole moment or the displacing of the ions between two equilibrium positions. For ferrite materials the dielectric relaxation mechanism is very sensitive to factors such as temperature, electric field, ionic substitution, structural defects, etc. The defects depend on either intrinsic or extrinsic heterogeneities due to special heat treatments, ionic substitutions, grains size additives and grain boundary nature [16]. On the other hand, structural defects may cause modifications of the short or long range interactions in ferrite materials [20].

Dielectric constant, is achieve from link, $C = \varepsilon_o \varepsilon \frac{A}{d}$ which *C, d, A* and *the area*s capacitance, thickness of the sample, area of the sample and permittivity of free space respectively [14]. This constant is produced while an occurrence of polarization in dielectrics during external field is applied. When dielectric material is placed between two parallel plates, the total charge between parallel plates increases. Instantly explain this constant depend on frequency of external electric field. The total charge between parallel plates increases are due to the polarization in the materials such as space charge polarization, bipolar polarization, ionic polarization and electronic polarization. Polarization type verification, which occurred in dielectric materials can be ensured when the existence of interaction between entities charges in dielectrics with external field frequency [21]. When the frequency of external electric field increase, there is the polarization that cannot follow the frequency of external electric field, so the certain polarization will be delayed. This polarization type can be verified based on relaxation frequency in frequency range studies.

Polarization mechanism in NZF can be explained by dielectric parameter like complex permittivity and dissipation tangent [14] in the frequency range of 10^{-2} Hz to 3 x 10^{6} Hz. This parameters dispersion on frequency shows the existence of interaction between external electric fields with charges in this frequency range [22]. Apart from that it gives a rough picture of polarization types that corresponds with processes of charges delay that have occurred in the frequency range studied [23]. Figure 4 shows the dielectric permittivity varies with frequency. At the low frequency distribution of variation is random is due to electrode polarization. At the frequency range in between 100 Hz to several thousand hertz, dielectric polarization produced when the vibration charge $Fe^{2+} \leftrightarrow Fe^{3+}$ and $Ni^{2+} \leftrightarrow Ni^{3+}$ follows the vibration of external electric field. When the frequency of external electric field increases, the charges vibration cannot follow the external electric field vibration and relaxation happen to its charges [10,14, 20]. These phenomena show the decreasing trend.

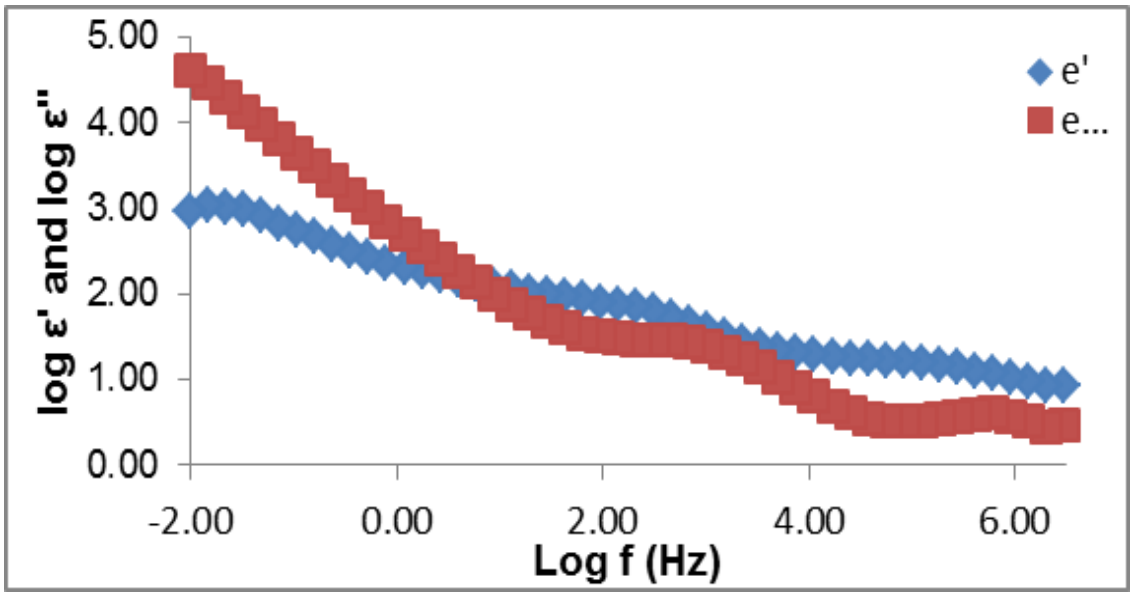

Figure 4: An example the variation of permittivity complex varies with frequency at temperature 303K of the sintered sample at 1573K

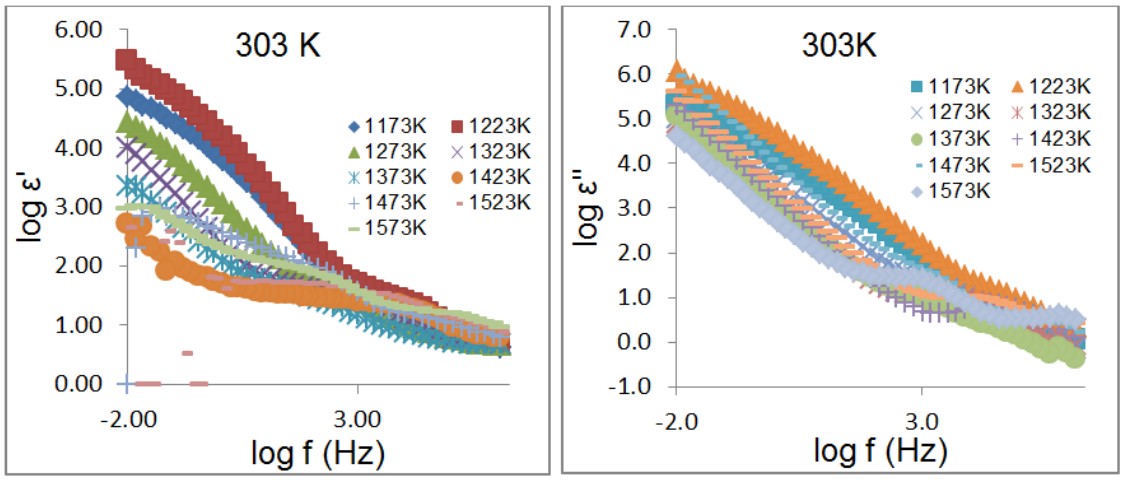

Figure 5: (a) The variety of real permittivity versus frequency from sintering temperature 1173 K to 1573 K (b) The variation of imaginary permittivity versus frequency from sintering temperature 1173 K to 1573 K

From Figure 5 (a) and 5 (b), the variation of ε' and ε'' versus frequency in the frequency ranges 10^{-2} Hz to 3 x 10^{6} Hz with sintering temperature in the range 1173 K to 1573 K. All the data were measured at 303 K. The variation of the real and imaginary permittivity versus frequency of each sintering temperature showed a decreasing trend and the variation are the random. This situation may occur from the changes in grain size drastically.

CONCLUSION

Microstructure of $Ni_{0.3}Zn_{0.7}Fe_2O_4$ from sintering temperatures 1173K to 1573K were successfully studied using X-ray diffraction and FESEM. The X-ray diffraction patterns confirm the synthesis of single crystalline phase of $Ni_{0.3}Zn_{0.7}Fe_2O_4$ nanoparticles and the grain size of surface samples were measured showing the grain size increasing drastically when sintering temperature increases. The activation energy of grain growth was calculated using the gradient of the slope of the graph and the value of each part are 205.0 ± 3.0 eV and 454.0 ± 3.0 eV respectively. Dielectric properties of the samples also discuss and showed the dielectric permittivity decreases when the frequency of external electric field increase. Interfacial polarization is dominant at low frequency contribute to increase the dielectric constant in frequency range studied.

ACKNOWLEDGEMENTS

Financial support of the Putra High Prestige Individual Grant vote 941180 and Ministry of Education Malaysian is gratefully acknowledged.

REFERENCE

[1] A. Dias, *Materials Research Bulletin* **35** 1439–1446 (2000)
[2] R.Valenzuela, Novel Applications of Ferrites, Hindawi Publishing Corporation, Physics Research International (2012), Article ID 591839, doi:10.1155/2012/591839.
[3] A. C. F. M. Costa, E. Tortella, M. R. Morelli and R. H. G. A. Kiminami, *J. Magn. Magn. Mater.* **256** 174-182 (2003)
[4] U. R. Lima, M. C. Nasar, R. S. Nasar, M. C. Rezende and J. H. Araujoc, *J. Magn. Magn. Mater.* **320** 1666-1670 (2008)
[5] A.M Abdeen, *J. Magn. Magn. Mater.* **192** 121-129 (1999)
[6] Y. Sahoo, A. Goodarzi, M. T. Swihart, T. Y. Ohulchansky, N. Kaur, E. P. Fulani and P. N. Prasad, *J. Phys. Chem. B.***109** (2005) 3879-3885
[7] P.B.C. Rao and S.P. Setty, *Inter. J. Engin. Sci. and Tech.* **2** (8) 3351-3354 (2010)
[8] I.H. Gul, W. Ahmed and A. Maqsood, *J. Magn. Magn. Mater.* **320** 270-275 (2008)
[9] N. Rezlesus and E. Rezlesus, *Physica Status Solidi*, **23** (2) 575-582 (1974)
[10] G. R. Mohan and D. Ravinder . *Materials letters* **40** 39-45 (1999)
[11] V. R. Kulkarani, M. M. Todhar and A. S. Vaingankar, *Indian J. Pure. Appl. Phys.* **24** 294 (1986)
[12] G. S. Shahane and K. V. Zipare, Structural, *International Journal of Science,* **1** (2) 12 – 15 (2012)
[13] K. R. Krishna, K. V. Kumar and D. Ravinder, *Advances in Materials Physics and Chemistry,* **2** 185 – 191 (2012)
[14] M. N. Mat, M. K. Halimah, W. M. Daud, H. Mansor and Y. Zainuddin. *Advanced Materials Research,* **1107** 59 – 64 (2015)
[15] M.P. Harmer, E.W. Roberts, R. Brook, *Trans Br Ceram Soc* **78** 22 (1979)
[16] K. Ishino and Y. Narumiya, *Am Ceram Soc Bull* **66** 1469 (1987)
[17] C. H. Lee, J. Hassan, M. Hashim, R. S. Aziz and N. M. Saiden, *International Journal of Research in Applied, Natural and Social Sciences,* **2** (5) 37 – 44 (2014)
[18] I. R. Idza, M. Hashim, N. Rodziah, I. Ismayadi and A. R. Norailiana, *Materials Research Bulletin* **47** 1145 – 1152 (2012)
[19] A. C. Hee, M. Mehrali, H. S. C. Metselaar and N. A. A. Osman, *Electronic Materials Letter,* **8** (6) 639 – 642 (2012)
[20] A. Dias and R. L. Moreira, *Materials Letters* **39** 69–76 (1999)
[21] M.N. Mat, W. Mahmood Mat Yunus, W. M. Daud W. Yusoff dan Zainul Abidin Hassan, *Pertanika J. Sci & Technol* **9** (2) 237 – 244 (2000)
[22] M.N. Mat, W. M.M. Yunus, W. M. Daud and A. H. Zainul, *Pertanika J. Sci. & Technol.* **11** (1) 9 – 16 (2003)
[23] L. Zhigao, J. P. Bonnet, J. Ravez, J. M. Reau and P. Hagenmuller, *J. Phys. Chem. Solids*, **53** (1) 1 – 9 (1992)
[24] K.Omar, M. D. J. Ooi and M. M. Hassin, *Modern Applied Science,* **3** (2) 110 – 116 (2009)